Appl. Phys. B 41, 173–178 (1986)

Applied Physics B Photophysics and Laser Chemistry

Coherent Anti-Stokes Raman Spectroscopy (CARS) of the ν_3 Band of Methane in Supersonic Molecular Beams

F. Huisken and T. Pertsch

Max-Planck-Institut für Strömungsforschung, Bunsenstrasse 10, D-3400 Göttingen, Fed. Rep. Germany

Received 16 May 1986/Accepted 30 June 1986

Abstract. Supersonic molecular beams of methane are investigated in the expansion region using coherent anti-Stokes Raman scattering (CARS). Raman spectra of the ν_3 vibration with resolved rotational structure at low temperatures are reported. Comparison with calculated CARS spectra shows that the rotational distribution in the beam may be well described by a Boltzmann distribution. Temperatures are the same for all three nuclear spin modifications within the experimental error.

PACS: 42.65, 33.20.Fb, 34.50.Ez

In recent years, coherent anti-Stokes Raman spectroscopy (CARS) has been shown to be an excellent and very versatile technique for spectroscopic studies in the expansion region of supersonic molecular beams. It has been successfully applied to the study of rotational relaxation processes for N_2, O_2, H_2, D_2, and C_2H_4 by Huber-Wälchli and Nibler (1) and for C_2H_2, C_2H_4, and CH_4 by Byer and coworkers [2–4]. Very recently we have studied the ν_3 vibration of NH_3 in a supersonic jet [5]. As an interesting result we found that the two nuclear spin modifications of ammonia relax at different rates.

The most thoroughly studied molecule using coherent Raman techniques is probably CH_4. Methane has four fundamental vibrations which are all Raman active and thus accessible to CARS spectroscopy. If, however, standard CARS techniques are employed the C–H stretching vibrations ν_1 and ν_3 are most conveniently investigated because of their large Raman shifts. Especially the ν_1 mode with its large Raman cross section has attracted much interest, but very high resolution lasers are needed to resolve individual rotational lines in the Q branch. In equilibrium cells such high resolution investigations have been reported by several authors using CARS [6–8] or other coherent Raman techniques like stimulated Raman gain [9] or inverse Raman [10] spectroscopy. The only studies involving molecular beams have been published by Byer and co-workers [3, 4] and Valentini et al. [11].

Much less work, especially in molecular beams, has been done as far as the ν_3 mode of methane is concerned. For this vibration the Raman cross section is a factor of two smaller [12] but, on the other hand, this mode has the advantage that commercially available lasers with moderate resolution can be used. There is one early CARS study of the ν_3 mode in a static cell by Nibler and Knighten [13] and one molecular beam investigation by Reuss and coworkers [14] employing conventional spontaneous Raman spectroscopy but no molecular beam CARS study has been published so far.

We have built a CARS spectrometer combined with a molecular beam machine. In this paper we give a first detailed description of the apparatus and report our results on the investigation of the ν_3 band of CH_4 in the expansion region of a supersonic jet at various distances. Finally, the measured CARS spectra are compared with calculations allowing us to determine rotational temperatures in the beam.

Experimental

A schematic view of the experimental setup is shown in Fig. 1. The CARS spectrometer consists of a frequency-doubled Nd:YAG laser (Quantel YG 481) delivering up to 400 mJ at 532 nm. Its output is split into two

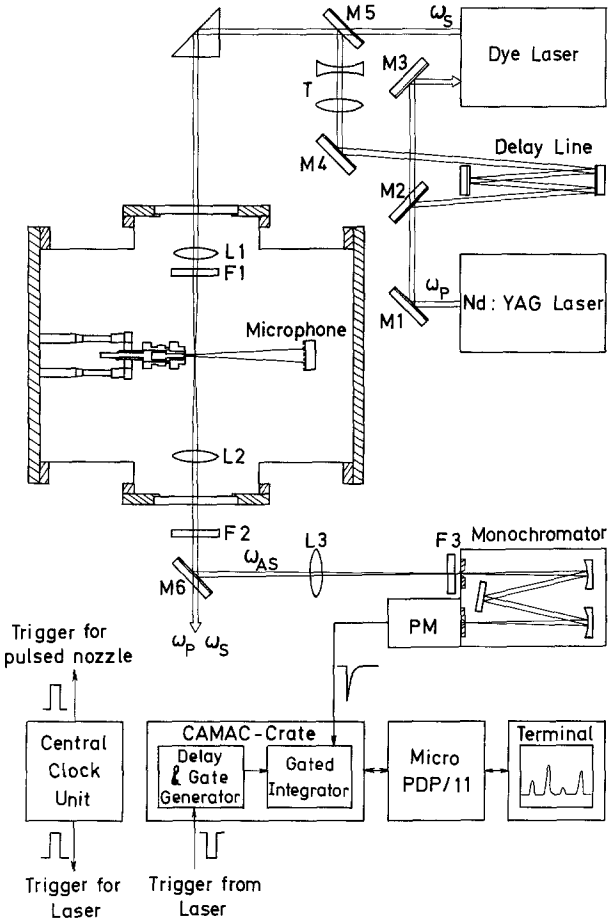

Fig. 1. Schematic view of the experimental setup

parts by means of a 12% reflecting beam splitter (M2). The transmitted beam is used to pump with 350 mJ a tunable dye laser (Quantel TDL IV). The other part provides the pump beam (ω_p) for the CARS process. After being time-delayed and attenuated to an adequate power level, it is reduced in diameter by a telescope (T) and combined with the output of the dye laser by means of a long wave pass dichroic mirror (M5; CVI LWP 5800). The dye laser is operated with Rhodamin 640 and provides the Stokes photons with frequency ω_s. Its output is also attenuated by means of neutral density filters. Typical pulse energies and bandwidths are 12 mJ and 0.12 cm^{-1} for ω_p and 6 mJ and 0.8 cm^{-1} for ω_s. The repetition rate is 10 Hz. Both laser beams are carefully aligned for optimum spatial overlap and enter the molecular beam machine through a quartz window.

The molecular beam machine consists of a cylindrical vacuum chamber 65 cm long and 30 cm in diameter. It is pumped by a 6000 l/s oil diffusion pump (Leybold Heraeus DI 6000), a 350 m^3/h roots pump (Alcatel RSV 350) and a 65 m^3/h rotary pump (Alcatel 2063). Since the vacuum obtained with the roots pump was good enough for our purpose the measurements reported here were carried out without operating diffusion pump. The pulsed molecular beam is formed by expanding the gas through the 1 mm diameter nozzle of a slightly modified automobile fuel injector (Bosch, model 0 280 150 035) kept at room temperature. The main modifications are as follows: 1) In order to provide a better leak tight seat the tip of the hardened metal plunger was replaced by a similarly shaped piece of teflon but without the small 1 mm diameter needle. 2) The front of the nozzle was ground off to a thickness of less than 0.2 mm at the 1 mm diameter hole. 3) The wire of the solenoid was replaced by a wire twice as thick as the original one in order to allow the solenoid to be operated at higher currents. 4) Finally the spring was replaced by a stronger one. The last two modifications serve to reduce both the opening and closing time. Similar pulsed nozzles based on conventional automobile fuel injection valves have been used previously [15–17].

The molecular beam source is mounted on a *xyz* translation stage and can be positioned during operation relative to the fixed laser beams. It is synchronized with the laser system and supplies gas pulses which can be adjusted in duration between 0.2 and 2 ms. Inlet pressures are varied between 1 and 8 atm. A miniature microphone (Knowles, model BT 1759) is used to monitor the pulsed molecular beam intensity and to optimize the timing between nozzle and laser.

The laser beams are focused onto the molecular beam axis by a $f = 100$ mm quartz lens (L1). Thus the probed volume is estimated to be a cylinder 1 mm long and less than 0.05 mm in diameter oriented perpendicular to the molecular beam axis. A yellow filter (F1; Schott GG 475) blocks any non-resonant blue light generated in air and the optical components or originating from the flashlamps of the Nd:YAG laser. Another lens (L2) with the same focal length as L1 is used to collect the blue anti-Stokes photons which, in the case of resonance, are generated by the nonlinear interaction of the lasers with the molecular beam. A filter (F2; Schott BG 3), a dichroic mirror (M6; CVI LWP 4900) and a bandpass filter (F3; Corion P10–460) separate the blue light from the generating laser beams. The anti-Stokes beam is then sent through a 0.3 m monochromator (McPherson, model 218) which serves as an additional filter and is finally detected by a photomultiplier (EMI, model 9813 B).

The CARS signal is processed by a minicomputer controlled boxcar integrator incorporated into a CAMAC [18] crate. Its heart is a gated integrator board (Evans Ass., model 4130) which has been built into a CAMAC module. The appropriate delay and gate are provided by a programmable CAMAC dual preset counter (Borer, model 1008) triggered by the laser. Since we chose an input resistor of 100 kΩ for the

gated integrator a gate of 60 μs was suitable. Another preset scaler of the same type is used to measure the integration time by counting the laser pulses. The output of the gated integrator, i.e. the integrated signal, is fed to a CAMAC analog to digital converter (Kinetic Systems, model 3553) and then transferred to the minicomputer (DEC Micro/PDP-11). The computer also controls the scanning of the dye laser via an appropriate interface (Quantel, ASC-2) and thus allows the automatic recording of CARS spectra. Typically, the signal is collected for 50 laser shots which corresponds to 5 s. During that time the dye laser is scanned quasi-continuously via a step motor with a speed of 0.002 nm/s. Therefore each data point in the measured spectra represents a signal integrated over 0.01 nm or 0.25 cm^{-1}, respectively. Although lowering the overall resolution this procedure has the advantage that very sharp peaks in the spectrum cannot be missed.

Results and Discussion

Figure 2 shows our CARS spectra of the ν_3 vibration as measured in the expansion region of a pulsed supersonic molecular beam of pure methane. The source has been kept at room temperature and the stagnation pressure was 1.5 atm at a 1 mm diameter nozzle. The distance between probing volume and nozzle exit has been varied between $x=0.5$ mm (upper spectrum) and $x=10$ mm (lowest spectrum). The various lines, as indicated in the upper spectrum, are assigned according to Berger [19]. Besides the ν_3 and $2\nu_2$ Q branches with unresolved rotational structure the R^+ and S^+ branches as well as the less intense R^0 and S^0 branches of the ν_3 vibration could be resolved. It is readily seen that the spectra become more and more simple as the distance is increased. Due to rotational relaxation the peaks corresponding to low rotational states gain in intensity at the expense of the higher states. At $x=10$ mm only the lowest three rotational states $j=0$ to $j=2$ can be observed proving that the rotational relaxation is very efficient in CH_4.

In order to get quantitative information about the rotational temperatures in the jet we have performed computer calculations. The theory of CARS has been covered in a number of excellent review articles [13, 20, 21]. They derive for the power $\mathscr{P}_{as}$ of the generated CARS beam

$$\mathscr{P}_{as}=c'\omega_{as}^2|\chi^{(3)}_{\mathrm{CARS}}|^2\mathscr{P}_p^2\mathscr{P}_s \tag{1}$$

where $\mathscr{P}_p$ and $\mathscr{P}_s$ are the power of the pump and Stokes beams with frequencies ω_p and ω_s. $\omega_{as}=2\omega_p-\omega_s$ is the frequency of the anti-Stokes beam and c' is a frequency independent constant. The third order suspectibility $\chi^{(3)}_{\mathrm{CARS}}$ consists of a nonresonant term χ_{nr} and a resonant

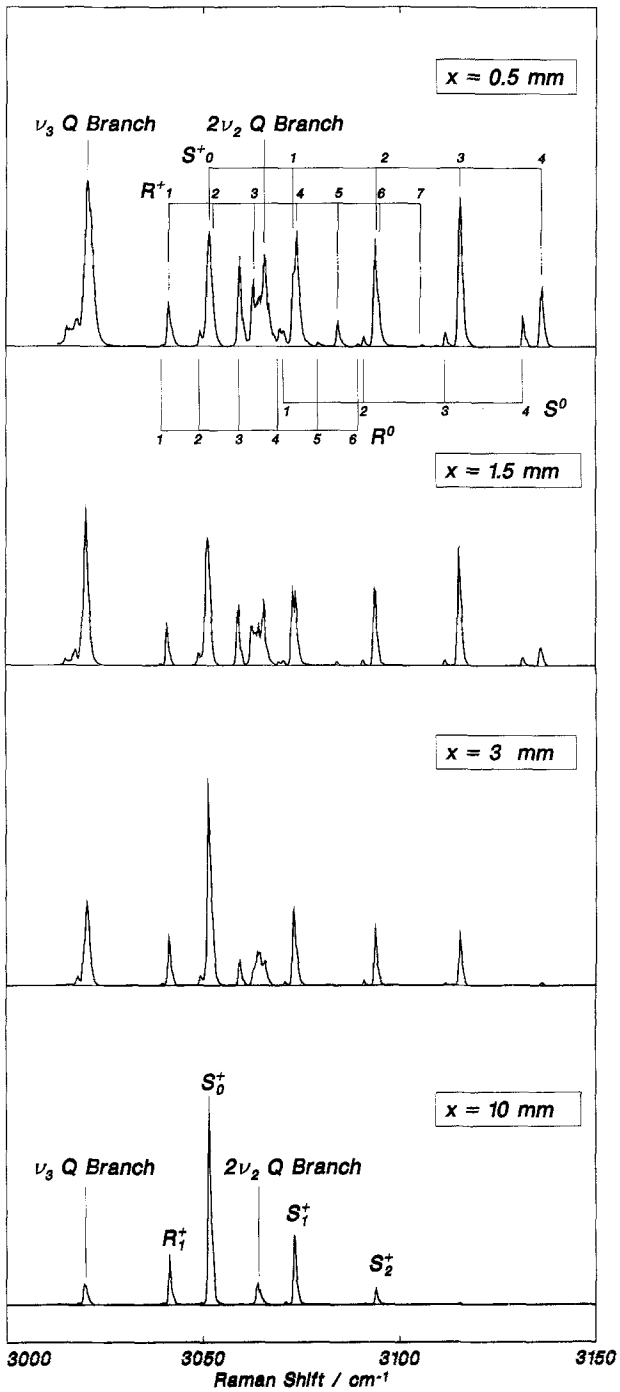

Fig. 2. Measured CARS spectra of the ν_3 vibration of CH_4 as a function of distance from the nozzle

contribution which is determined by the characteristic properties of the molecule

$$\chi^{(3)}_{\mathrm{CARS}}(\omega_s)=\chi_{nr}+\frac{Nc^4}{\hbar\omega_s^4}\left(\frac{d\sigma}{d\omega}\right)\frac{1}{\omega_0-(\omega_p-\omega_s)-i\Gamma/2}. \tag{2}$$

In this formula the Raman transition is characterized by its frequency ω_0, its full width at half maximum

(FWHM) Γ and its differential cross section $d\sigma/d\omega$. Normally N is the difference in population between lower and upper states but since in our molecular beam the upper vibrational state is not populated N is just the number of molecules in the lower state.

If several transitions are very close they may contribute to the CARS signal altogether and (2) has to be replaced by a sum where the summation is taken over all participating states. We assume that due to the vacuum environment and low density in the molecular beam the nonresonant term χ_{nr} is small and can be neglected compared to the resonant contribution. Moreover we take into account the specific properties of the ν_3 Raman band of methane and thus we obtain

$$\chi^{(3)}_{\mathrm{CARS}}(\omega_s)=c''\omega_s^{-4}\sum_{JT\Delta}\frac{P_T(J)\,\beta(\Delta,J,T)}{\omega_{\Delta,J}-\omega_p+\omega_s-\mathrm{i}\Gamma/2}. \tag{3}$$

Here T designates the nuclear spin modification of CH_4 ($T=A$, E or F) and the index Δ characterizes the branch which is regarded (e.g., S^+, S^0, S^-, R^+, R^0, R^-, ...). $P_T(J)$ is the probability of finding the molecule as species T in the rotational state J. If we assume that the rotational distribution in the beam can always be described by a Boltzmann distribution and if we further assume that collision induced transitions between the different nuclear spin modifications A, E and F are not allowed $P_T(J)$ can be written as a function of the rotational temperature T_{rot}

$$P_T(J)=a_T\frac{g_T(J)\,(2J+1)\exp[-hc\,F_0(J)/kT_{\mathrm{rot}}]}{\sum_{J'}g_T(J')\,(2J'+1)\exp[-hc\,F_0(J')/kT_{\mathrm{rot}}]}. \tag{4}$$

Here a_T is the natural abundance of the modification T at 300 K ($a_T=5/16$, $2/16$, $9/16$ for $T=A$, E, F) and $g_T(2J+1)$ the statistical weight of the rotational level as tabulated in Herzberg's Table 7 [22].

In (3) the Raman cross sections have been replaced by Raman coefficients $\beta(\Delta, J, T)$. They are calculated for the ν_3 band of methane by Herranz and Stoicheff [23]. As a consequence of centrifugal distortion each rotational state splits into $2J+1$ sublevels each designated by the index $\tau=nT$. Since we cannot resolve this splitting our $\beta(\Delta, J, T)$ is obtained by summing over all final and averaging over all initial states, i.e.

$$\beta(\Delta,J,T)=f(\Delta,J)\,N_n^{-1}\sum_{nn'}(b_J(\Delta))_{nT,n'T}, \tag{5}$$

where $(b_J(\Delta))_{nT,n'T}$ are the coefficients and $f(\Delta, J)$ the functions as tabulated in [Ref. 23, Tables 2 and 3]. N_n is the number of levels of species T in the vibrational ground state. The averaging over the initial states is necessary if the statistical weights of Herzberg [22] are used. Thus our Raman coefficients are identical to those of Reuss and co-workers [14].

Combining (1 and 3) and taking into account that the power of the laser beams has been kept constant during the experiment we finally obtain for the power of the CARS signal

$$\mathscr{P}_{as}(\omega_s)=c'''\omega_{as}^2\omega_s^{-8}\left|\sum_{JT\Delta}\frac{P_T(J)\,\beta(\Delta,J,T)}{\omega_{\Delta,J}-\omega_p+\omega_s-\mathrm{i}\Gamma/2}\right|^2, \tag{6}$$

where c''' is another constant.

In order to compute the complete CARS spectrum we proceed as follows: According to (6) we calculate the CARS signal in the range between 3000 and 3150 cm^{-1} taking into account the four branches $\Delta=S^+$, R^+, S^0, and R^0 and rotations from $J=0$ to $J=9$. The line positions $\omega_{\Delta,J}$ are taken from [19]. Although the true width is around 0.01 cm^{-1} [8], for the sake of faster computation, Γ is chosen to be 0.1 cm^{-1}. This value is not critical since, in order to account for the limited resolution of the laser system, the whole spectrum is finally convoluted with a Gauss function of full width at half maximum γ. Best results are obtained with $\gamma=0.9\ \mathrm{cm}^{-1}$. This value compares favourable with the overall resolution that we calculate from the laser specifications and scan parameters to be approximately $\sqrt{0.12^2+0.8^2+0.25^2}=0.85\ \mathrm{cm}^{-1}$.

The rotational temperature T_{rot} which determines the rotational state distribution $P_T(J)$ according to (4) is varied until best agreement with the measured spectra is obtained. Figure 3 shows a comparison between the measurement at $x=3$ mm and the calculation based on a rotational temperature $T_{\mathrm{rot}}=45$ K. Aside from the ν_3 and $2\nu_2$ Q branches which have not been considered in the calculation because of their unresolved rotations the agreement is quite good. It should be noted, however, that the ratio of the S^+ to R^+ branch peaks given by the theory did not agree with the measurement. In order to get a satisfactory fit we had to multiply all CARS intensities of the R^+ branch by a factor of 1.25.

The good agreement within a single branch proves that the rotational distribution in the beam is thermal and can be very well described by a Boltzmann distribution. These findings are in contrast to the results of some authors [24, 25] who found athermal distributions in molecular beams of N_2 and HF. In the calculation, we have also admitted different rotational temperatures for the different modifications A, E, and F but, within the experimental error, we obtained satisfactory results if we assumed a unique temperature for all three species. This again is in contrast to our findings with ammonia [5] where we found a significant lower temperature for the A modification and also to the results of Reuss and co-workers [14] who found, although not very significantly, slightly different temperatures for the A and F modifications of CH_4.

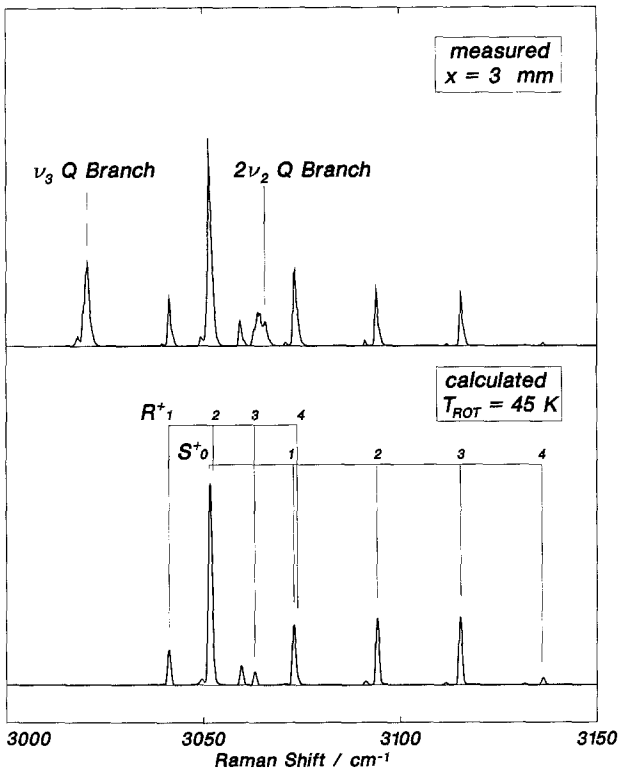

Fig. 3. Comparison between measured and calculated CARS spectra

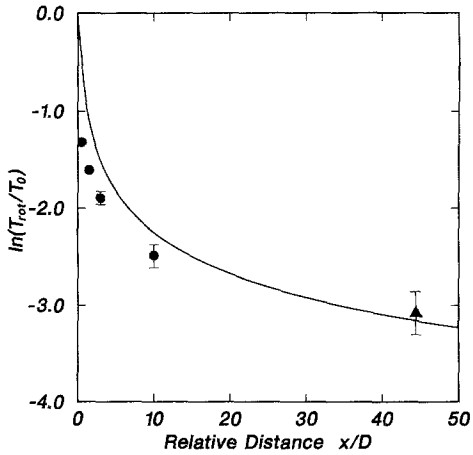

Fig. 4. The rotational temperature T_{rot} versus x/D. The solid curve crorresponds to the isentropic expansion. Full circles are obtained with the pulsed nozzle, the triangle is the results of a measurement in a continuous molecular beam

In the same way we have fitted all measured spectra presented in Fig. 2. Thus we can assign a rotational temperature T_{rot} to each measured distance. For $x=10$ mm we determine a rotational temperature $T_{rot}=25$ K. At this position almost all molecules have relaxed into their respective ground states $J=0$ for the A, $J=1$ for the F and $J=2$ for the E modification. For complete relaxation one would expect a ratio of 100:59.6:1.6 for the CARS intensities of the lines S_0^+, S_1^+, and S_2^+.

The dependence of the rotational temperature on the distance from the nozzle is displayed in Fig. 4. Here the logarithm of T_{rot}/T_0 (T_0:nozzle temperature:300 K) is plotted against the reduced distance x/D (D:nozzle diameter: 1 mm). The solid curve represents the calculation for an ideal isentropic expansion [26] of CH_4. As a striking and unexpected feature we notice that our rotational temperatures which are represented by full circles are significantly lower than calculated for an ideal expansion. This behaviour can be explained by assuming that the expansion starts already a few nozzle diameters before the nozzle exit. As a result our x/D values should be corrected and shifted towards larger values. But it is also very likely that the specific geometry of the source is responsible for the observed fast cooling. It is possible that the metal plunger inside the nozzle is not sufficiently drawn back and that a small channel is formed. This would cause a precooling of the gas so that the temperature T_0 is lower than 300 K at the nozzle exit. The consideration of this effect would yield higher reduced temperatures T_{rot}/T_0.

In order to prove that our determination of the rotational temperatures is not responsible for the observed discrepancies we have also investigated a continuous molecular beam of methane. The nozzle diameter in this experiment was 45 μm and the backing pressure 50 atm. At a distance of 2 mm from the nozzle, i.e. $x/D=44.4$, we determine a rotational temperature of 14 ± 3 K. This value is plotted in Fig. 4 with a triangle and lies slightly above the isentropic curve. It indicates that the rotational temperature is slightly higher than the translational temperature calculated for an ideal expansion as is expected and reasonable.

Conclusion

Our results demonstrate that CARS is a valuable tool for studying rotational relaxation processes in the expansion region of molecular beams. We have shown that already moderate resolution lasers are very well suited to obtain rotationally resolved information about the relaxation of methane in a supersonic jet. By fitting theoretical spectra to the measurements rotational temperatures could be assigned to various positions in the jet. Our results indicate that the rotational distribution can be well described by a Boltzmann distribution and that the temperatures are the same for all three modifications of CH_4. That the rotational temperatures are lower than expected for an ideal expansion is attributed to the specific geometry of the pulsed nozzle.

Our measurements further demonstrate that, due to rotational cooling, molecular beams can be success-

fully employed to significantly simplify complicated spectra. Another exciting application of CARS combined with molecular beams is the study of van der Waals complexes as they are formed in the expansion region of supersonic jets. First studies on C_2H_4Ar clusters [27] as well as HCN [28] and CO_2 [29] complexes have already been reported and very recently we have measured CARS spectra of NH_3 clusters which will be published shortly [30].

Acknowledgement. The computer calculations have been executed and the spectra have been plotted at the 'Gesellschaft für wissenschaftliche Datenverarbeitung' (GWD) in Göttingen.

References

1. P. Huber-Wälchli, J.W. Nibler: J. Chem. Phys. **76**, 273 (1982)
2. M.D. Duncan, P. Österlin, R.L. Byer: Opt. Lett. **6**, 90 (1981)
3. R.L. Byer, M. Duncan, E. Gustafson, P. Oesterlin, F. König: In *Laser Spectroscopy V*, ed. by A.R.W. McKellar, T. Oka, and B.P. Stoicheff, Springer Ser. Opt. Sci. **30** (Springer, Berlin, Heidelberg 1981) pp. 233–241
4. E.K. Gustafson, R.L. Byer: In *Laser Spectroscopy VI*, ed. by H.P. Weber and W. Lüthy, Springer Ser. Opt. Sci. **40** (Springer, Berlin, Heidelberg 1983) pp. 326–329
5. F. Huisken, T. Pertsch: Chem. Phys. Lett. **123**, 99 (1986)
6. H. Frunder, D. Illig, H. Finsterhölzl, H.W. Schrötter, B. Lavorel, G. Roussel, J.C. Hilico, J.P. Champion, G. Pierre, G. Poussigue, E. Pascaud: Chem. Phys. Lett. **100**, 110 (1983)
7. D.N. Kozlov, A.M. Prokhorov, V.V. Smirnov: J. Mol. Spectrosc. **77**, 21 (1979)
8. J.P. Boquillon, R. Bregier: Appl. Phys. **18**, 195 (1979)
9. A. Owyoung, C.W. Patterson, R.S. McDowell: Chem. Phys. Lett. **59**, 156 (1978)
10. A. Owyoung: In *Laser Spectroscopy IV*, ed. by H. Walther and K.W. Rothe, Springer Ser. Opt. Sci. **21** (Springer, Berlin, Heidelberg 1979) pp. 175–187
11. J.J. Valentini, P. Esherick, A. Owyoung: Chem. Phys. Lett. **75**, 590 (1980)
12. H.W. Schrötter, H.W. Klöckner: In *Raman Spectroscopy of Gases and Liquids*, ed. by A. Weber, Topics Cur. Phys. **11** (Springer, Berlin, Heidelberg 1979) pp. 123–166
13. J.W. Nibler, G.V. Knighten: In *Raman Spectroscopy of Gases and Liquids*, ed. by A. Weber, Topics Cur. Physic. **11** (Springer, Berlin, Heidelberg 1979) pp. 253–299
14. G. Luijks, S. Stolte, J. Reuss: Chem. Physics **62**, 217 (1981)
15. F.M. Behlen, N. Mikami, S.A. Rice: Chem. Phys. Lett. **60**, 364 (1979)
16. C.E. Otis, P.M. Johnson: Rev. Sci. Instrum. **51**, 1128 (1980)
17. D. Bassi, S. Iannotta, S. Niccolini: Rev. Sci. Instrum. **52**, 8 (1981)
18. CAMAC is an internationally accepted interface standard (ANSI/IEEE-583, IEC-640) and stands for Computer Automated Measurement and Control. For specifications see for example: Euratom Report EUR 4100e, Luxemburg (1972)
19. H. Berger: J. Mol. Spectrosc. **66**, 55 (1977)
20. W.M. Tolles, J.W. Nibler, J.R. McDonald, A.B. Harvey: Appl. Spectrosc. **31**, 253 (1977)
21. S.A.J. Druet, J.P. Taran: Progr. Quant. Electr. **7**, 1 (1981)
22. G. Herzberg: *Molecular Spectra and Molecular Structure*, Vol. 2 (Van Nostrand, New York 1945) p. 39
23. J. Herranz, B.P. Stoicheff: J. Mol. Spectrosc. **10**, 448 (1963)
24. S.P. Hernandez, P.J. Dagdigian, J.P. Doering: Chem. Phys. Lett. **91**, 409 (1982)
25. T.E. Gough, R.E. Miller: J. Chem. Phys. **78**, 4486 (1983)
26. J.B. Anderson: In *Molecular Beams and Low Density Gasdynamics*, ed. by P.P. Wegener (Dekker, New York 1974) pp. 1–91
27. F. König, P. Oesterlin, R.L. Byer: Chem. Phys. Lett. **88**, 477 (1982)
28. G.A. Hopkins, M. Maroncelli, J.W. Nibler, T.R. Dyke: Chem. Phys. Lett. **114**, 97 (1985)
29. G.A. Pubanz, M. Maroncelli, J.W. Nibler: Chem. Phys. Lett. **120**, 313 (1985)
30. H.D. Barth, F. Huisken: To be published